Selective-field-ionization dynamics of a lithium $m=2$ Rydberg state: Landau-Zener model versus quantal approach

M. Førre[1,2] and J. P. Hansen[3]
[1]*Department of Physics, University of Bergen, Allègt. 55, N-5007, Norway*
[2]*Laboratoire de Chimie Physique-Matière et Rayonnement, Université Pierre et Marie Curie, 11, rue Pierre et Marie Curie, 75231 Paris Cedex 05, France*
[3]*Department of Physics, Po. 7800, University of Bergen, Norway*
(Received 10 February 2003; published 28 May 2003)

The selective-field-ionization (SFI) dynamics of a Rydberg state of lithium with magnetic quantum number $m=2$ is studied in detail based on two different theoretical models: (1) a close coupling integration of the Schrödinger equation and (2) the multichannel (incoherent) Landau-Zener (MLZ) model. The $m=2$ states are particularly interesting, since they define a border zone between fully adiabatic ($m=0,1$) and fully diabatic ($m>2$) ionization dynamics. Both sets of calculations are performed up to, and above, the classical ionization limit. It is found that the MLZ model is excellent in the description of the fully diabatic dynamics while certain discrepancies between the time dependent quantal amplitudes appear when the dynamics become involved. Thus, in this region, the analysis of experimental SFI spectra should be performed with care.

DOI: 10.1103/PhysRevA.67.053402 PACS number(s): 32.80.Rm, 33.80.Rv, 33.60.−q

I. INTRODUCTION

The method of selective-field ionization (SFI) has been studied thoroughly both theoretically and experimentally for several decades [1,2]. SFI methods are now mature and well known experimental procedures to measure detailed quantal state-to-state dynamics. The method is in particular useful for characterization of the population distribution of highly excited states in atoms and molecules. Intrashell dynamics of hydrogenlike Rydberg atoms in weak electric and magnetic fields [3,4], collisions between slow ions and Rydberg atoms [5], manipulation of quantum entanglement of atoms and photons in a cavity [6], and, more recently, observation of cold antihydrogen [7] are examples where the SFI technique has been used to characterize the Rydberg level population.

The principle of SFI is simply to expose the Rydberg atoms to a time-dependent increasing (ramped) electric field. Depending on the specific state, atoms in different quantum states will ionize at different field strengths. The electrons are accelerated by the field and hit a detector, which produce a signal. In this way a SFI spectrum as a function of the field (time) is plotted. In alkali Rydberg atoms, which are used in most experiments, the level crossings between low angular momentum states show avoided crossings in the region of inter-n mixing in contrast to the exact crossings in hydrogenic Rydberg atoms. With a typical ramping field (400–1000 V/cm/μs) one usually considers $|m|=0,1$ states of lithium to traverse the avoided crossings adiabatically, whereas $|m|\geqslant 2$ states pass the crossings diabatically. The SFI technique does usually not distinguish between $m=0$ and $m=\pm 1$ states since they for all practical purposes traverse the avoided crossings adiabatically with the field ramps specified above, and field ionize at the classical ionization limit $E\sim(16n^4)^{-1}$ a.u. This is sometimes referred to as adiabatic field ionization. But the technique clearly distinguishes these states from $m>2$ states, which traverse the crossings plainly diabatically and field ionize at the hydrogenic ionization limit (the nonclassical ionization limit), at much higher fields.

Recently, it has been pointed out that $|m|=2$ states may also have an adiabatic component [4,8]. A ''mixed'' dynamics, as suggested here, will then require particular care in the analysis of the spectra and from a theoretical point of view the validity of simple models should be investigated in detail. Most theoretical attempts to study the SFI process have been carried out in the extreme case where the evolution becomes purely diabatic or adiabatic after a few avoided crossings. However, a few more thorough theoretical works have been done on the system [2,8,9], but they are all treated within the multichannel Landau-Zener (MLZ) approximation.

The main purpose of this paper is to carry out a first detailed study of the dynamics of various $m=2$ states of the Li ($n=25$) Stark manifold when exposed to a realistic time-dependent increasing electric field. The degree of adiabaticity/diabaticity of these states is studied in detail and the results of the MLZ model are confronted with *ab initio* time-dependent quantal calculations. The behavior of such a complex quantum system and its route from a localized bound state towards breakup is interesting in its own right. However, in the present study the main motivation is to investigate the dynamics of the transition zone between fully diabatic and fully adiabatic field ionization in relation to the interpretation of experiments [4]. Atomic units ($\hbar=e=m_e=1$) are used throughout except where units are given explicitly.

II. THEORETICAL MODELS

A. Numerical model

The Hamiltonian of a pseudo-one-electron alkali-metal Rydberg atom in a homogeneous time-dependent electric field is given by

$$H=H_0+V_c(r)+F_z(t)z, \tag{1}$$

where $H_0=-\nabla^2/2-1/r$ and $V_c(r)$ are the unperturbed hydrogenic Hamiltonian and the perturbation due to the core, respectively. Spin-orbit effects may safely be ignored for the lighter Rydberg atoms, i.e., for H, Li, and Na [1,10].

The core potential is set up by the induced correction to the Coulomb potential resulting from the interaction between the excited electron and the inner shell electrons. The perturbation is assumed to be significant for low angular momentum states only, since high angular momentum states are prohibited from penetration into the core region. In the core region the effect on the Rydberg electron is a more strongly attractive force, which mainly accounts for a positive phase shift of the hydrogenic radial functions [11]. For highly excited states of the field free Hamiltonian the radial functions outside the core are accurately described by the Bates-Damgaard-type quantum defect radial wave functions [12]. These functions are basically hydrogenic wave functions with the nodes phase shifted inward. The field free energy levels are modified according to

$$W_{nl}=-\frac{1}{2(n-\delta_{nl})}, \tag{2}$$

where δ_{nl} are the so-called quantum defects, which break the degeneracy of the energy levels. For high n values the quantum defects become almost energy independent [1,13], and for the Rydberg states of lithium the nonvanishing quantum defects take the values [1] $\delta_s=0.3995$, $\delta_p=0.0472$, $\delta_d=0.0021$, and $\delta_f=0.0003$.

Because of spherical symmetry of the core potential the wave function may be expanded in hydrogenlike wave functions in the region outside the core [4,10,14]. In the present work it is more suitable to choose an expansion in ordinary hydrogenic wave functions,

$$\Psi(r,t)=\sum_{nlm} c_{nlm}(t)R_{nl}(r)Y_{lm}(\theta,\phi), \tag{3}$$

to take advantage of known procedures for analytic calculation of matrix elements [15]. The wave function expansion is inserted into the Schrödinger equation $i(\partial/\partial t)\Psi(r,t)=H\Psi(r,t)$, leading to a first-order coupled matrix system of equations for the expansion coefficients, $c_{nlm}(t)$,

$$i\frac{d}{dt}\vec{c}=\mathbf{M}(t)\vec{c}. \tag{4}$$

Within the first-order perturbation theory the core induces couplings [1,16],

$$\langle nlm|V_c(r)|n'l'm'\rangle=\frac{-\delta_l}{\sqrt{n^3n'^3}}\delta_{ll'}\delta_{mm'}, \tag{5}$$

between the hydrogen nlm spherical states with the same l and m quantum numbers. This approximation is excellent for the highly excited states of interest in the present work.

The nonvanishing matrix elements of the z operator follow within the dipole approximation the selection rules $\Delta l=\pm 1$, $\Delta m=0$. Since $z=r\cos\theta=\sqrt{(4\pi/3)}rY_{10}$, the angular part of the matrix element is straightforward calculated by using the Wigner-Eckart theorem for spherical harmonics [17], with the well-known result,

$$\langle lm|\cos\theta|l-1m\rangle=\left(\frac{l^2-m^2}{(2l+1)(2l-1)}\right)^{1/2}. \tag{6}$$

The radial part of the dipole matrix elements, $\langle nl|r|n'l-1\rangle$, is either found by direct numerical integration or is given in terms of the hypergeometric function $F(a,b,c,d)$ [18],

$$\begin{aligned}\langle nl|r|n'l-1\rangle=&\frac{(-1)^{n'-l}}{4(2l-1)!}\sqrt{\frac{(n+1)!(n'+l-1)!}{(n-l-1)!(n'-l)!}}\\&\times\frac{(4nn')^{l+1}(n-n')^{n+n'-2l-2}}{(n+n')^{n+n'}}\\&\times\left[F\left(-n+l+1,-n'+l,2l,-\frac{4nn'}{(n-n')^2}\right)\right.\\&-\left(\frac{n-n'}{n+n'}\right)^2F\left(-n+l-1,-n'+l,2l,\right.\\&\left.\left.-\frac{4nn'}{(n-n')^2}\right)\right].\end{aligned} \tag{7}$$

The formula is valid for $n\neq n'$. Within one principal shell the expression is in particular simple,

$$\langle nl|r|nl-1\rangle=-\tfrac{3}{2}n\sqrt{n^2-l^2}. \tag{8}$$

Since the core potential exclusively couples states of equal m quantum numbers due to the spherical symmetry of the potential, and since the z operator obeys the $\Delta m=0$ selection rule, it is sufficient to expand the Schrödinger equation on a basis set consisting only of m states identical to the initial m values.

B. Analytical multichannel Landau-Zener model

The dynamics will be compared with an incoherent MLZ model [19]. Let $\vec{P}(t)=[P_1(t),P_2(t),\ldots,P_n(t),\ldots]$ be the probability distributions on the eigenstates at each time t. As a bookkeeping device the probability corresponding to each state is chosen to be ordered with increasing energy in $\vec{P}$, i.e., the state with lowest energy always comes first in the vector. We use the hydrogenic parabolic states $\{|nn_1n_2m\rangle\}$ as a basis set and calculate the couplings by formula [1],

$$\begin{aligned}\langle nn_1n_2m|V_c(r)|n'n_1'n_2'm\rangle=&\sum_l\langle nn_1n_2m|nlm\rangle\\&\times\frac{-\delta_l}{\sqrt{n^3n'^3}}\langle n'lm|n'n_1'n_2'm\rangle.\end{aligned} \tag{9}$$

The crossing times t_i (i.e., the times where the diabatic energy curves cross) for each Landau-Zener crossing, and the information about which two states that cross at each t_i, are found from the expression for the eigenenergies within second-order perturbation theory in the electric field [18],

$$W(n,n_1,n_2,m) = -\frac{1}{2n^2} + \frac{3}{2}n(n_1-n_2)\gamma t - \frac{1}{16}n^4\gamma^2 t^2 \times [17n^2 - 3(n_1-n_2)^2 - 9m^2 + 19], \tag{10}$$

where γ is the slew rate (slope) of the electric field. Let P_i (P_j) and P_i' (P_j') be the population probability of the adiabatic state i (j) before and after the crossing point is passed, respectively. The Landau-Zener model then gives

$$\begin{pmatrix} P_i' \\ P_j' \end{pmatrix} = \begin{pmatrix} 1-P_{LZ} & P_{LZ} \\ P_{LZ} & 1-P_{LZ} \end{pmatrix} \begin{pmatrix} P_i \\ P_j \end{pmatrix}, \tag{11}$$

where P_{LZ} is the two-state Landau-Zener probability for a diabatic passage (nonadiabatic transition) through the crossing points. The two-state probability is given by [20],

$$P_{LZ} = e^{-2\pi(d^2/a)}, \tag{12}$$

where a is the absolute difference in slope of the two diabatic eigenenergy curves at the crossing [calculated from the derivative of Eq. (10)], and d is the coupling from Eq. (9). Within the first-order perturbation theory in the field both a and d are constant, i.e., an almost ideal situation for application of the Landau-Zener model.

C. Ionization probability

Since our basis set only includes bound states, the numerical solution of the Schrödinger equation does not automatically give any information about the field strength needed to ionize the states. To obtain an estimate of the ionization probability we use the semiempirical formula for the ionization rate of hydrogen derived by Damburg and Kolosov [21],

$$\Gamma = \frac{(4R)^{2n_2+m+1}}{n^3 n_2!(n_2+m)!}\exp\left[-\frac{2}{3}R - \frac{1}{4}n^3F\left(34n_2^2 + 34n_2m + 46n_2 + 7m^2 + 23m + \frac{53}{3}\right)\right], \tag{13}$$

where $R=(-2W)^{3/2}/F$ and F is the electric field. The Stark energy W is calculated by a perturbation expansion up to fourth order in the field [22]. They claim that this formula is correct within a precision of a few percent for the threshold field for ionization of the different states. This accuracy is more than sufficient for the present analysis. We have tested the formula on the data in Fig. 4 of Robicheaux, Wesdrop, and Noordam [2], and it successfully reproduced the position of all the peaks in the SFI spectrum calculated in that work.

Assuming a one way exponential decay into the continuum the survival probability takes the form

$$P_{surv} = \exp\left(-\int_{t_0}^{t}\Gamma(t')dt'\right). \tag{14}$$

III. RESULTS

The electric field is ramped linearly from an initial field

$$F(t) = F_0 + \gamma t, \tag{15}$$

where F_0 is chosen arbitrarily but weak enough to avoid intershell mixing, i.e., $F_0 \ll 1/3n^5$. For the present field ramps the spin-orbit effects at zero field are ignorable [1], hence F_0 can likely be put to zero. Four different values of the ramp, $\gamma = 100,421,1000,$ and 10,000 V/cm/μs, have been tried. These values correspond to relatively slow to ultrafast switching with respect to experimental applicable ranges. For field strengths less than 1000 V/cm and with the initial population distribution within the $n=25$ manifold, the energy spectrum of the system appears to be sufficiently converged for a basis set including the manifolds from $n=21$ to $n=40$. It may seem strange and even wrong to solve this huge and complex system numerically by using a basis set only including bound hydrogenic states since the eigenstates that decrease in energy with increasing field, in fact, are continuum states immediately after the field is turned on. What saves us is that, despite being continuum states, they behave as bound states all the way up to the classical ionization limit, i.e., in the energy region [23],

$$W \leqslant -2\sqrt{F} + |m|F^{3/4} + \frac{3}{16}m^2F. \tag{16}$$

Thus, one should be aware that the calculations may be less accurate in the region close to the classical ionization limit. For further details on the discussion of the applicability of using a truncated basis set see Ref. [10].

Figure 1 shows the quantum dynamics of the parabolic states $|nn_1n_2m\rangle = |25\,23\,0\,1\rangle$ and $|nn_1n_2m\rangle = |25\,21\,0\,3\rangle$ for a 421 V/cm/μs field ramp. It is clearly seen that the $m=3$ state follows a completely diabatic development, whereas the time development of the $m=1$ state is plainly adiabatic. In the latter case the population spreads out to a band of states. The formation of a narrow band can be understood from the Landau-Zener model as P_{LZ} rapidly falls to zero in the region outside the adiabatic state in the center of the band. All states in the band will ionize near the classical ionization limit, whereas the state $|25\,21\,0\,3\rangle$ ionizes at the hydrogenic ionization limit at very strong fields.

Now turning to the $m=2$ case we display in Fig. 2 the time development of the initial $|25\,22\,0\,2\rangle$ state for the same parameters as in Fig. 1. Here, a mixed evolution, which is neither diabatic nor adiabatic, is observed. The first crossings with the states belonging to the principal shell above are, however, traversed completely diabatically. As new red states from above are reached d increases, whereas a decreases, i.e., P_{LZ} decreases and the dynamics become more and more adiabatic. At crossings with the state $|26\,8\,15\,2\rangle$, the adiabatic leakage becomes visible (as green) in the figure. As the $n=27$ levels enter the dynamics, giving the first triple cross-

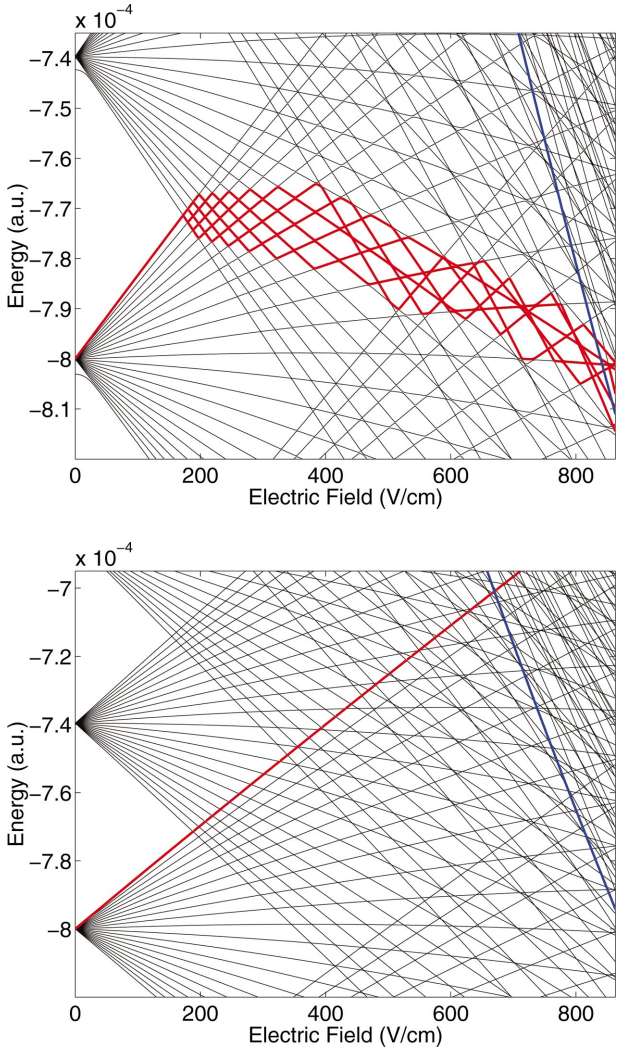

FIG. 1. (Color) The SFI dynamics of two initial parabolic states $|25\,23\,0\,1\rangle$ (upper) and $|25\,21\,0\,3\rangle$ (lower) for a 421 V/cm/μs field ramp in the lithium $|m|=1$ and $|m|=3$ Stark energy spectrums, respectively. In both cases the part of the eigenenergy spectrum, which corresponds to states with significant population probability, i.e., probability greater than 0.5 percent, is marked. The classical ionization limit is shown as a blue line.

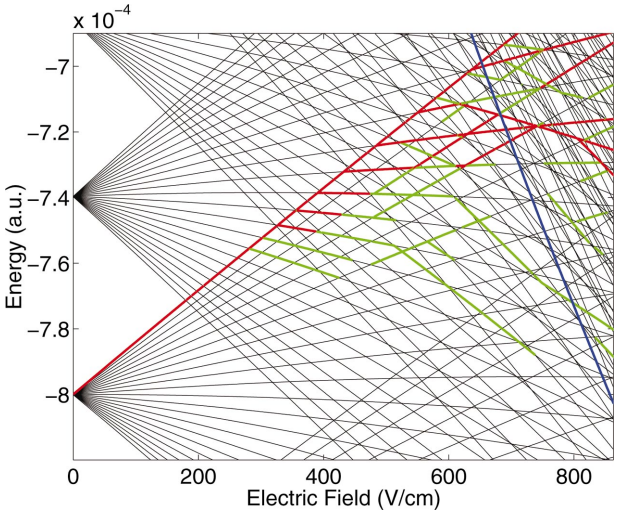

FIG. 2. (Color) The SFI dynamics of the parabolic state $|25\,22\,0\,2\rangle$ in a 421 V/cm/μs field ramp. The part of the eigenenergy spectrum, which corresponds to states with population probability $P>1\%$, is plotted in red, whereas states with $0.5\% \leqslant P \leqslant 1\%$ are shown in green. The classical ionization limit is shown as a blue line.

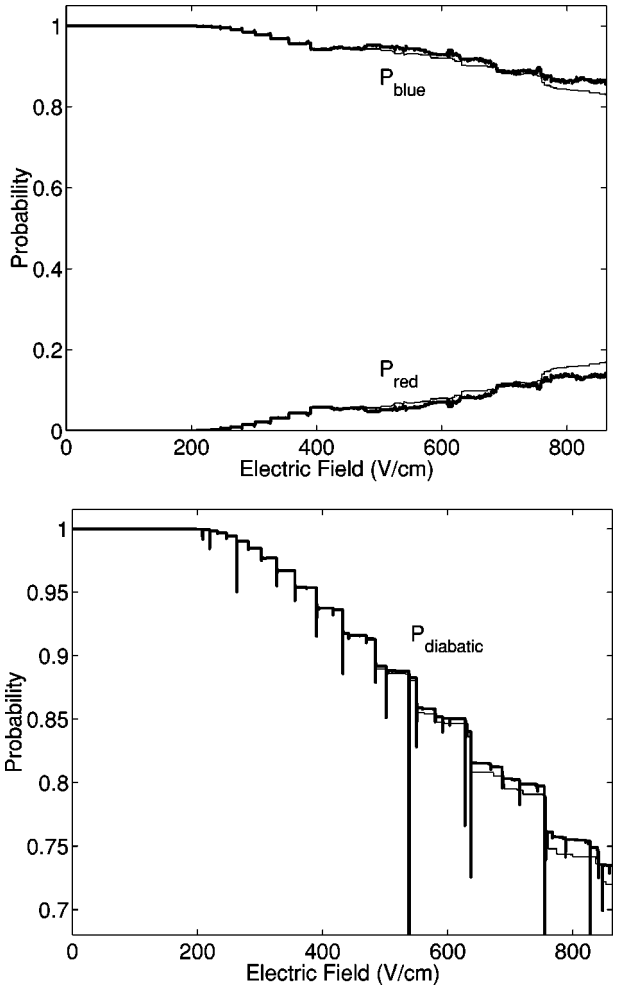

FIG. 3. A plot of P_{blue}, P_{red}, and $P_{diabatic}$ for the parabolic state $|25\,22\,0\,2\rangle$ in a 421 V/cm/μs field ramp.

ings, there is a significant sharing of probabilities between the adiabatic and diabatic directions for each new crossing (shown in red). The time the various paths reach their ionization limit varies and as a result an experimental SFI spectrum may contain a broad distribution.

We use the notation of Refs. [1,18] and define the states where the electron is most likely located on the side of the atom away from the saddle point as blue states, and the states with the electron located adjacent to the saddle point as red states. Blue and red states are characterized by the eigenenergy curves in the Stark spectrum going upward and downward, respectively. Roughly speaking one expects the red states to ionize near the classical ionization limit, whereas the blue states ionize at much higher field. But, in general, this subdivision into two groups is not satisfactory, as the decay rate function, Eq. (13), is a continuous function on n_2.

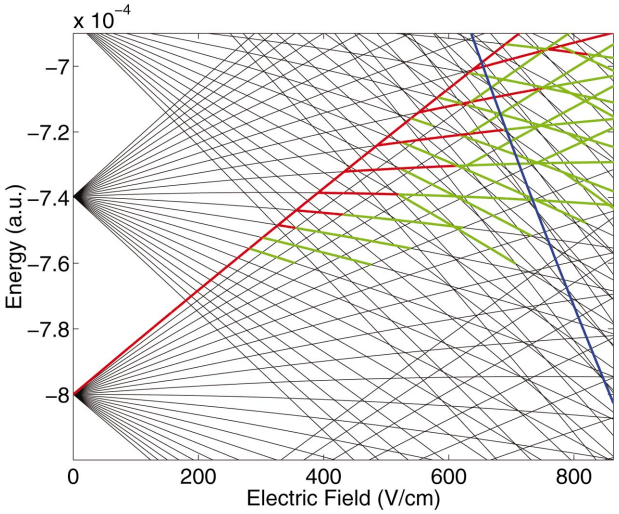

FIG. 4. (Color) The MLZ results for the SFI dynamics of the parabolic state $|25\,22\,0\,2\rangle$ in a 421 V/cm/μs field ramp. Notation as in Fig. 2.

Let P_{blue} and P_{red} be the total population in blue and red states, respectively. Define also $P_{diabatic}$ to be the probability for the initial state to traverse all the avoided crossings completely diabatically. P_{blue}, P_{red}, and $P_{diabatic}$ are plotted in Fig. 3 for the initial state $|25\,22\,0\,2\rangle$. The uppermost Stark state in the $n=25$ manifold is the state with the highest diabatic component. Figure 3 shows that more than 25% of this initial blue state has been transferred to other channels at the classical ionization limit ($\sim$850 V/cm), about 15% to red states and the rest to other blue states. Formula (14) estimates a probability more than 15% for this blue state to ionize within 1 μs. For the lower lying states in the manifold the ionization probability is even higher. This prediction of ionization probability for the $|25\,22\,0\,2\rangle$ state is sufficient to explain the observed discrepancies between the experimental and calculated data in Ref. [4].

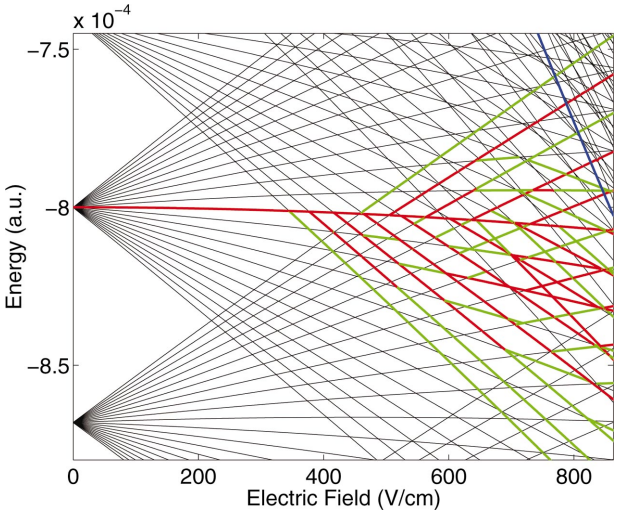

FIG. 5. (Color) Same as Fig. 2 for an initial state $|25\,11\,11\,2\rangle$, with green and red color corresponding to $0.5\% \leqslant P \leqslant 3\%$ and $P > 3\%$, respectively.

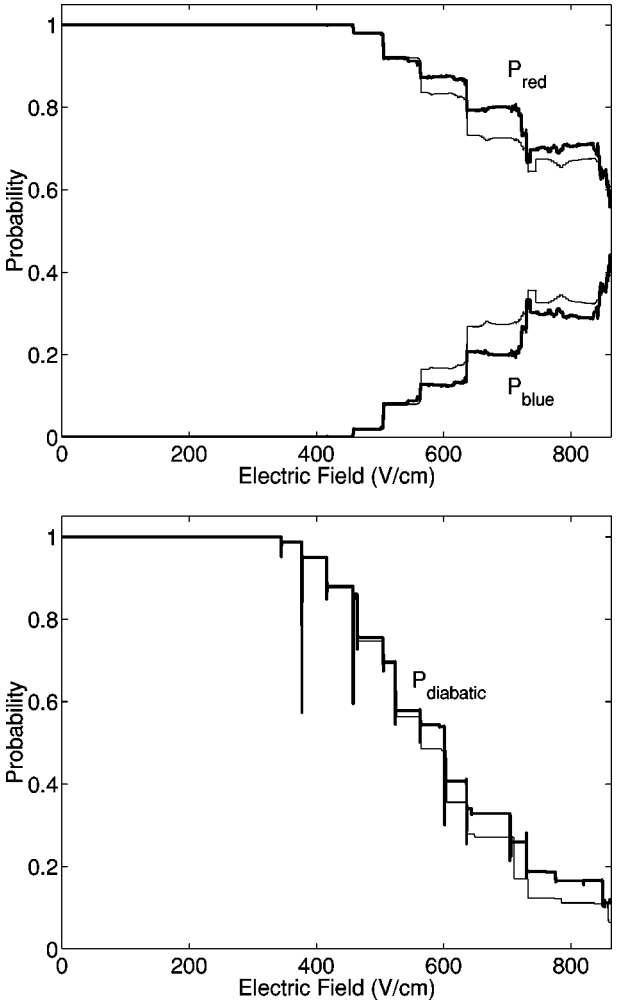

FIG. 6. Same as Fig. 3 for an initial state $|25\,11\,11\,2\rangle$.

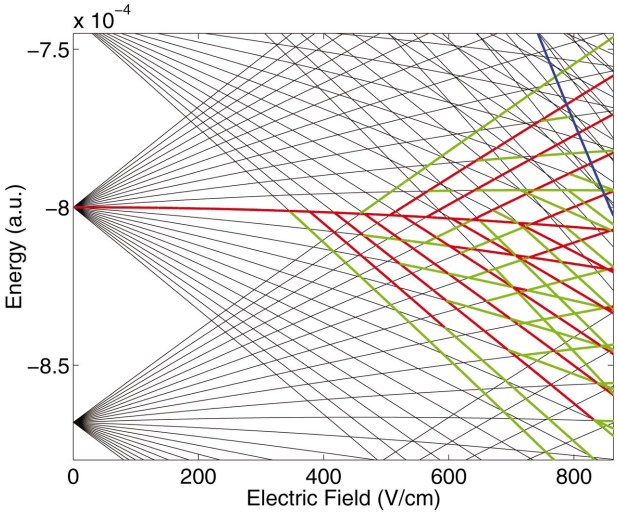

FIG. 7. (Color) The MLZ results for the SFI dynamics of the parabolic state $|25\,11\,11\,2\rangle$ in a 421 V/cm/μs field ramp. Notation as in Fig. 5.

For comparison, the MLZ calculations are also shown in Fig. 3. The MLZ behavior of the red and blue population dynamics is seen to be in good agreement with the quantal calculations. The dramatic spikes of the initial state, however, are time dependent in their origin and related to phase development and therefore clearly not reproduced in the incoherent MLZ approach. For the special situation with one single initial state selected in the uppermost (or lowermost) part of the $n=25$ manifold, the probability of remaining in the initial diabatic state is completely independent of the phases of different paths, because the diabatic energy level at most crosses the same adiabatic energy level once. This explains the agreement between the numerical and the MLZ calculations in Fig. 3.

In Fig. 4 we plot the corresponding MLZ dynamics of Fig. 2. At this level certain discrepancies become evident: Some of the channels are less populated, especially in the adiabatic ''direction,'' whereas others are more populated. Thus, even if the total population in ''blue'' and ''red'' states is the same in both models, the time of ionization will differ and create different ''theoretical SFI spectra.'' The observed deviations for higher fields ($F>500$ V/cm) are believed to originate from higher-order corrections to the energy that are neglected in the Landau-Zener model. Phase interference effects, and also a possible breakdown in the validity of the Landau-Zener model as the level crossings become very dense, can also play a role. To avoid confusion note that the basis set for the Landau-Zener calculations is truncated for a less extensive basis set than for the fully numerical calculations. This only affects the number of visible eigenenergy curves above the classical ionization limit, and not the dynamics. The degree of agreement in Figs. 2–4 raises the question whether the state-to-state dynamics is accurately described by the MLZ model. However, one should be aware of the fact that in this example only very few states have a population probability greater than 1 percent throughout the dynamics. Hence, from the beginning phase interference effects are expected to play a minor role.

Figure 5 gives an example of an initial state in the middle of the manifold. For this case the adiabaticity of the crossings becomes significantly higher, and the population is spread more efficiently out on the other states in the energy spectrum. Hence, in contrast to the dynamics of the first case, phase interference effects are expected to play a stronger role. There are two immediate differences between the spectra in Figs. 2 and 5: First, the crossings start later for the latter case, i.e., at the field $F\sim 350$ V/cm instead of $F\sim 180$ V/cm. Second, the multiple number of avoided crossings between the initial (diabatic) $|25\,11\,11\,2\rangle$ state and the same adiabatic neighbor state both above and below this diabatic state, respectively, opens the possibility of influences from the dynamical phase not only in the network of states, but also in the fully diabatic development of the initial $|25\,11\,11\,2\rangle$ state.

In Fig. 6 the red/blue probabilities are again shown and compared with the MLZ model. At first sight a fairly good agreement is still present, which is surprising since the phase is expected to play a significant role in the population dynamics. There are, however, important differences at the crossings for $F>500$ V/cm. The figure shows that in the regions $F\sim 525$ V/cm, $F\sim 560$ V/cm, $F\sim 640$ V/cm, and $F>700$ V/cm, there are clear discrepancies in the strength of the population jumps. It is interesting to note that these regions coalesce with the regions of the energy spectrum where three or more states are crossing. This indicates that phase effects are in action. Despite that the MLZ result deviates significantly in certain regions, the overall picture is that the MLZ result is not diverging from the exact quantum calculations. Thus the present calculations strengthen the assumption made by the authors of Ref. [2]: The phase accumulation on the different paths cancel because of the very large number of ways for the population to choose up to the ionization limit. This is confirmed in Fig. 7, where the MLZ network dynamics is shown. The degree of spreading is rather similar with the quantal calculation in Fig. 5. Some differences in the relative population strength of various paths are, however, still present. As in the case of the initial $|25\,22\,0\,2\rangle$ dynamics, it is therefore fair to conclude that this may lead to different final spectra.

Let t_i $(i=1,2,\ldots)$ define the times [calculated from Eq. (10)] when the hydrogenic energy level of a given initial state $|nn_1n_2m\rangle$ crosses with the other parabolic energy levels in the energy spectrum. The corresponding couplings introduced when lithium is considered are found from Eq. (9) in terms of Clebsch-Gordan coefficients. Then the total probability of remaining in the initial state, i.e., the probability of traversing the avoided crossings completely diabatically, may be estimated by the simple formula

$$P=\prod_{t_i} p_i, \tag{17}$$

where $p_i=\exp(-2\pi d_i^2/a_i)$ is the Landau-Zener probability of diabatic passage through each Landau-Zener crossing at time t_i. Now a criteria for diabatic evolution with time becomes

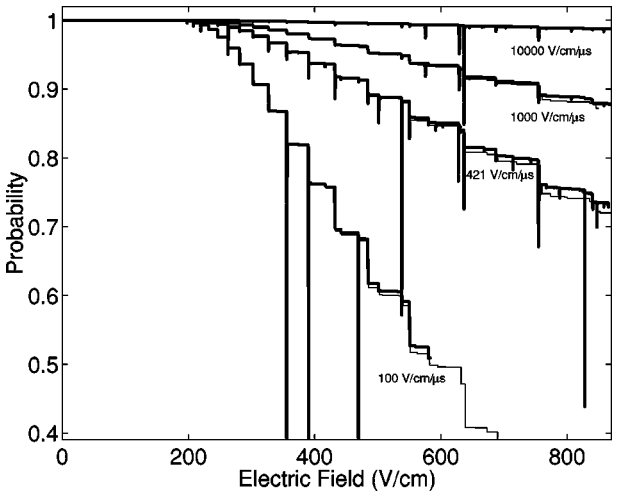

FIG. 8. The probability $P_{diabatic}$ of traversing all the avoided crossings completely diabatically for the parabolic state $|25\,22\,0\,2\rangle$ for four different electric field ramps: 100 V/cm/μs, 421 V/cm/μs, 1000 V/cm/μs, and 10 000 V/cm/μs. The thin lines give the corresponding results from the MLZ model.

$P \sim 1$. Formula (17) is expected to be less accurate for eigenstates in the middle of the manifold because of coherences, as discussed above.

Figure 8 shows the probability of remaining in the initial extreme Stark state $|25\,22\,0\,2\rangle$ as a function of time for different electric field ramps. It shows that a ramp of the order of 10 000 V/cm/μs is needed in order to make this state traverse the crossings plainly diabatically. For the lower lying states in the manifold the adiabatic component will be even more significant. Surprisingly the curves representing different field ramps are more or less linear as a function of the electric field. And the slope seems to depend on one single parameter only, i.e., the slew rate of the ramp. This may be understood from the MLZ model. Define the slope between the crossings at field strengths F_{i-1} and F_i by

$$\lambda \equiv \frac{P(F_i) - P(F_{i-1})}{F_i - F_{i-1}}. \tag{18}$$

Assume that p_i $(i=1,2,\ldots)$ is small, i.e., $p_i \simeq 1 - 2\pi d_i^2/a_i$. Harmin showed that the Clebsch-Gordan coefficients in the coupling can be written as [24] $\langle nn_1n_2m|nlm\rangle = \sqrt{2/n}(-1)^l P_{lm}((n_1-n_2)/n)$, where P_{lm} is the normalized associated Legendre polynomial [18]. From this we find that d is a very slowly decreasing function of $(n_1'-n_2')^2$ for $|n_1'-n_2'| \ll n'$ (marked variables always refer to the states which the population couples to). We consider only transitions to states in the manifold above. These are anyhow the most important for the adiabatic behavior. Then for $|n_1'-n_2'| \ll n'$ Eq. (18) can be approximated,

$$\lambda \simeq K\frac{1}{\gamma}, \tag{19}$$

where K is a constant, i.e., λ^{-1} is approximately proportional to γ for intermediate values of the field strength. This is in complete agreement with the result of Fig. 8.

IV. CONCLUSION

In the present paper we have carried out large basis close coupling calculations as well as multichannel Landau-Zener calculations on the ionization mechanism of a Li $(n=25)$ atom when exposed to an electric field. All in all a high degree of agreement between the results of a direct propagation of the time-dependent Schrödinger equation and the MLZ model is achieved, in contrast to what one very often observes in collision physics [19]. The calculations confirm that initial $m=2$ states behave neither diabatic nor adiabatic but ionize along a complex path resulting in a broad SFI spectrum. A detailed state-to-state comparison between the quantal and the MLZ dynamics have shown certain discrepancies. This suggests that corresponding detailed experimental interpretation must be performed with care, and most preferably in parallel with quantal calculations. Our calculations have also documented that the ramp speed of the electrical field has to be very fast if a full diabatic ionization shall occur. Further work based on a numerical grid solution of the Schrödinger equation, to accurately evolve the system from the classical field ionization limit up to where the atom is fully ionized, is in progress.

ACKNOWLEDGMENTS

We would like to thank D. Fregenal, L. Nyvang, E. Horsdal-Pedersen, and S. Selstø for useful discussions. This research was supported by NFR and Notur.

[1] T. F. Gallagher, *Rydberg Atoms* (Cambridge University Press, Cambridge, 1994).
[2] F. Robicheaux, C. Wesdorp, and L.D. Noordam, Phys. Rev. A **62**, 043404 (2000).
[3] D. Fregenal, T. Ehrenreich, B. Henningsen, E. Horsdal-Pedersen, L. Nyvang, and V.N. Ostrovsky, Phys. Rev. Lett. **87**, 223001 (2001).
[4] M. Førre, D. Fregenal, J.C. Day, T. Ehrenreich, J.P. Hansen, B. Henningsen, E. Horsdal-Pedersen, L. Nyvang, O.E. Povlsen, K. Taulbjerg, and I. Vogelius, J. Phys. B **35**, 401 (2002).
[5] L.G. Gray and K.B. MacAdam, J. Phys. B **27**, 3055 (1994).
[6] J.M. Raimond, M. Brune, and S. Haroche, Rev. Mod. Phys. **73**, 565 (2001).
[7] G. Gabrielse, N.S. Bowden, P. Oxley, A. Speck, C.H. Storry, J.N. Tan, M. Wessels, D. Grzonka, W. Oelert, G. Schepers, T. Sefzick, J. Walz, H. Pittner, T.W. Hänsch, and E.A. Hessels, Phys. Rev. Lett. **89**, 213401 (2002).
[8] D.A. Harmin and P.N. Price, Phys. Rev. A **49**, 1933 (1994).
[9] D.A. Harmin, Phys. Rev. A **56**, 232 (1997).
[10] M.L. Zimmerman, M.G. Littman, M.M. Kash, and D. Kleppner, Phys. Rev. A **20**, 2251 (1979).
[11] U. Fano, Comments At. Mol. Phys. **10**, 223 (1981).
[12] D.R. Bates and A. Damgaard, Philos. Trans. R. Soc. **22**, 101 (1949).
[13] M.J. Seaton, Mon. Not. R. Astron. Soc. **118**, 504 (1958).
[14] O.G. Larsen and K. Taulbjerg, J. Phys. B **17**, 4523 (1984).
[15] H. M. Nilsen, (unpublished).
[16] I.V. Komarov, T.P. Grozdanov, and R.K. Janev, J. Phys. B **13**, 573 (1980).
[17] D. M. Brink and G. R. Satchler, *Angular Momentum* (Oxford University Press, Oxford, 1968).
[18] H. A. Bethe and E. E. Salpeter, *Quantum Mechanics of One- and Two-Electron Atoms* (Springer-Verlag, Berlin, 1957).
[19] M.F.V. Lundsgaard, S.E. Nielsen, H. Rudolph, and J.P. Hansen, J. Phys. B **31**, 3215 (1998).
[20] C. Zener, Proc. R. Soc. London, Ser. A **137**, 696 (1932).
[21] R.J. Damburg and V.V. Kolosov, J. Phys. B **12**, 2637 (1979).
[22] H.J. Silverstone, Phys. Rev. A **18**, 1853 (1978).
[23] M.G. Littman, M.M. Kash, and D. Kleppner, Phys. Rev. Lett. **41**, 103 (1978).
[24] D. A. Harmin, in *Atomic Excitation and Recombination in External Fields*, edited by M. H. Nayfeh and C. W. Clark (Gordon and Breach, New York, 1985).